Single Gold Atoms Stabilized on Nanoscale Metal Oxide Supports are Catalytic Active Centers for Various Reactions

Chongyang Wang, Ming Yang, and Maria Flytzani-Stephanopoulos
Dept. of Chemical and Biological Engineering, Tufts University, Medford, MA 02155

DOI 10.1002/aic.15134
Published online December 29, 2015 in Wiley Online Library (wileyonlinelibrary.com)

Key recent findings that demonstrate that single-gold atom sites stabilized on various oxide supports by –O bonds are the unique catalytic sites for a number of reactions, including the water-gas shift reaction, methanol partial oxidation and steam reforming reactions, and the selective dehydrogenation of ethanol are summarized herein. Atomic dispersion of gold on various metal oxides was followed with aberration-corrected high angle annular dark field/scanning transmission microscopy imaging and x-ray absorption spectroscopy (XANES/EXAFS). Gold nanoparticles and subnanometer clusters are active only through their interfacial atoms directly interacting with the support, hence if present, they entail precious metal waste. From a design perspective, the important feature in these supported catalysts is the creation of many single-site gold species anchored on the oxide support to maximize activity. Atomic gold-centered catalyst designs afford 100% atom efficiency, and more importantly, have distinct product selectivity, different from that of extended metal surfaces. Novel experimental synthesis methods of atomically dispersed Au catalysts are discussed, which pave the way for the efficient use of precious metals, broadening the application of properly designed gold and other precious metals (Pt, Pd) to different reactions in energy conversion and green chemicals production. *AIChE J*, 62: 429–439, 2016
Keywords: gold, single atom catalysts, water-gas shift reaction, methanol steam reforming, ethanol dehydrogenation

Introduction

From the pioneering work of Giuseppe Parravano on the surface reactivity of supported gold in the early 1970s[1] to the demonstration of very high activity of supported gold nanoparticles for the CO oxidation reaction by Haruta and his coworkers in the late 1980s,[2] and the flurry of activity by researchers worldwide since that time, the case has been made for gold, inactive in bulk form, but very active and selective for a large number of reactions if present in special structural forms on a variety of supports. The list of reactions catalyzed by nanoscale gold is still growing. Following the work of Haruta et al.[3,4] on metal oxide (e.g., Fe_2O_3, TiO_2, NiO, and Co_3O_4) nanoscale gold catalysts, Liu et al.[5,6] have shown gold to be active when supported on CeO_2 both for the CO and the CH_4 complete oxidation reactions. Supported Au/CeO_2 was first reported by Fu et al.[7] in 2001 as a powerful new catalyst for the water-gas shift (WGS) reaction, while its attributes for the CO-preferential oxidation (PROX) reaction were reported by Deng et al.[8] in 2005. Until the demonstration of the activity of individual gold atoms, anchored as cation Au-O_x on ceria, for these reactions in 2003,[9] it was thought that the size of gold nanoparticles was the most important design parameter. It is fair to say, however, that Haruta had recognized as the important locus of activity the interface between the gold nanoparticles and the support,[2–4] but it was unclear whether these "perimetric" gold-support sites were unique to gold or included the oxide support as part of the active site. In much of the work that has followed these early studies, the role of the support as a ligand (through –O bonds) to gold atoms has been elucidated, as can be followed in the 2012 review by Flytzani-Stephanopoulos and Gates[10] which covers atomically dispersed supported metal catalysts, including gold, and the 2013 overview of supported gold atoms for the low-temperature WGS reactions by Flytzani-Stephanopoulos.[11] This body of work complements the general concept and realization of single-site heterogeneous catalysts advanced by Sir Meurig Thomas.[12] It should be noted at the outset that each metal atom (cation) thus stabilized on oxide supports retains its chemical "signature," for example Pt atoms on ceria and Au atoms on ceria have different intrinsic catalytic activity for the WGS reaction[9]; while Au atoms on CeO_2,[13] FeOx,[14,15] TiO_2,[16] La_2O_3,[17] and so forth, all have the same intrinsic activity[11] for this reaction. Therefore, the support identity does not matter. Of course, the support properties are crucial in providing enough anchoring sites to the metal atoms, thus increasing the total catalyst activity.[18] When an "inert" support, such as silica, zeolite, or carbon is used, addition of alkali oxides has been found to form the metal atom-centered, stabilized Pt-O_x[19–23] or Au-O_x[24] sites, with identical intrinsic activity as on "active" reducible oxide supports. Figure 1 shows the common activity (TOF) of atomically dispersed gold catalysts on a variety of supports for the WGS reaction.

The above brief account of atomic Au-O_x species as the active sites for the WGS and the PROX reactions, leads to the

Correspondence concerning this article should be addressed to M. Flytzani-Stephanopoulos at mflytzan@tufts.edu.

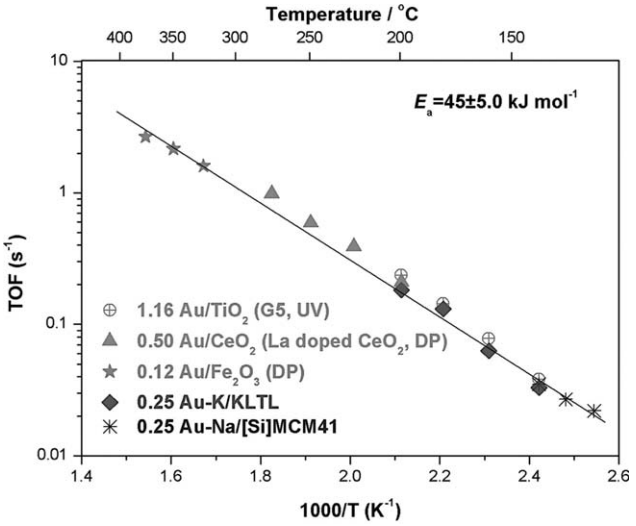

Figure 1. TOF plot for the WGS reaction over gold catalysts with atomically dispersed gold in a simulated reformate gas mixture (11% CO- 26% H_2O- 7% CO_2- 26% H_2-He).

Reprinted with the permission from Ref. 24. Copyright 2014 Science AAAS.

plausible question as to whether these species are the active sites for other reactions of interest to fuel conversion processes, for example, the hydrogen production via steam reforming of alcohols, or to the production of chemicals via the selective dehydrogenation reactions of alcohols. In this article, we examine two such reaction systems, namely: the steam reforming of methanol (SRM) and the selective dehydrogenation of ethanol on atomic Au-O_x sites stabilized on various supports. Gold was recently investigated as a catalyst for the SRM reaction by Yi et al.[25,26] who were first to report its high activity and selectivity for this reaction using 1 at.% gold deposited on nanoscale CeO_2. The selectivity is not limited by the WGS reaction, and these workers demonstrated that the reaction mechanism is through the oxidative self-coupling of methanol to methyl formate, which is hydrolyzed to formic acid, and the latter gives the final products CO_2 and H_2. In this scheme no CO is produced, and the selectivity to H_2 is maximized. These findings are in agreement with reports from the surface science literature on the partial oxidation of methanol on oxidized Au(111) surfaces[27] and the same reaction on nanoporous gold,[28] where methyl formate was the exclusive product formed. Boucher et al.[29,30] deposited 1 at.% gold on nanoscale ZnO with various shapes (rods, cubes, and polyhedra) and found it to be active for the SRM reaction. The intrinsic activity of Au-O_x was the same on either CeO_2 or ZnO supports. The potential shape effect of the support was investigated on both supports.[25,26,29,30] It was found that single crystal nanoshapes were more or less effective in anchoring the atomic gold species, thus affecting the overall catalyst activity. Certain facets (CeO_2{110, 111}, ZnO{0001}) are superior in dispersing gold than CeO_2{100} or ZnO{0110}), therefore, use of supports with predominantly the former surfaces would lead to superior catalyst activity. Limited by the fact that Zn and Au have overlapping excitation region in XANES/EXAFS measurements, the direct evidence of atomic dispersion of gold on the ZnO nanostructures was only through aberration-corrected high angle annular dark field/scanning transmission microscopy (ac-HAADF/STEM), which also identified other structures of gold (nanoclusters, nanoparticles) present on the ZnO nanorods and nanopolyhedra. Use of highly alkaline NaCN solutions to leach out the weakly bound gold particles, while it works well for CeO_2, is unsuitable for ZnO which also dissolves in these solutions. Also, the bulk ZnO nanoshapes could not be prepared with high surface areas to increase the number of anchored Au-O_x sites. For ZnO and also for TiO_2 supports, it became clear that a different gold preparation method was necessary. Only Au/CeO_2 was easy to prepare with high (0.5–1.0 wt.%) gold content as long as nano CeO_2 and La-doped nano CeO_2, with high density of oxygen vacancies, was used. CeO_2 is unique in stabilizing a large number of atomic gold species on its surface, similar to the well-studied Pt-group metals supported on CeO_2, and dispersing gold atomically on CeO_2 is less sensitive to the synthesis method (coprecipitation, deposition/precipitation, etc.) used. Using other supports, however, requires a suitable preparation method that will both make efficient use of gold precursors as well as result in large amounts of stabilized gold atoms on their surfaces.

Two new supported gold systems (Au/TiO_2 and Au/$ZnZrO_x$) are discussed in this article, using preparation techniques that maximize the number of anchored atomic gold species. In the case of TiO_2, a UV-assisted deposition/precipitation method is used to create Ti-O_x-Au anchoring sites and minimize the amount of gold forming nanoparticles. This type of material (with 1 wt.% Au atomically dispersed on the anatase surface) was shown to have high activity and stability for the WGS reaction by Yang et al.[16] It is examined here as catalyst for the SRM reaction. The composite $ZnZrO_x$ oxide is interesting as it contains well dispersed ZnO in the ZrO_2 domains, thus effectively giving high surface area to ZnO. Gold was deposited on it and applied as catalyst for the SRM reaction in recent work by Wang et al.[31] Further structural information was collected recently and is reported in this article. The $ZnZrO_x$ composite can be further used as a platform material with tunable surface acidity depending on the extent of the modification of the zirconia acid properties by the presence of ZnO.[32] The Au-O_x species on this support are shown to retain their chemical signature in the SRM reaction, and also catalyze the selective dehydrogenation of ethanol to acetaldehyde and hydrogen at low temperatures.

Synthesis of Atomically Dispersed Au-O(OH)$_x$− Species on TiO_2 and $ZnZrO_x$ Supports

Design and formulation of these two new gold catalysts introduces novel methods to achieve the atomic dispersion of gold and, in the case of the ZnO-containing catalyst, to achieve limited resistance toward leaching in highly alkaline solutions. Previous work by Boucher et al.[29,30] has demonstrated that nanoscale ZnO, in the form of truncated ZnO polyhedra presenting a majority of {0001} polar surfaces, is a good catalyst support of gold for the SRM[29] reaction. Abundant exposed ZnO {0001} surfaces with O step edge atoms from the ZnO nano-polyhedra have been reported to anchor gold through the Au-O_x-ZnO linkages via charge transfer between the gold atoms and the oxygen defects.[33] To prove that the Au-O_x-ZnO sites are the active ones for SRM, gold particles and clusters must be removed from the surface. As

mentioned above, the solubility of ZnO in high pH (>12) solutions limits the precise quantitation of Au atoms by NaCN leaching, because gold atomically bound on the ZnO will also be lost in the solution. Therefore, a new catalyst support that comprises defect-rich ZnO nano-domains dispersed on a support-like ZrO_2 may provide a surface more resistant to leaching in NaCN solutions. Motivated by recent reports by the Yong Wang's group,[32,34] a nanoscale composite metal oxide consisting of ZnO and ZrO_2 is synthesized by the carbon hard-template method, which involves coimpregnation of zinc and zirconium salt solutions onto the carbon followed by air calcination at 550°C to combust off the carbon template, leaving only a porous $ZnZrO_x$ material behind. This method results in ZrO_2 nanoparticles (~4 nm) with ZnO species homogeneously dispersed in the composite oxide both in the bulk and on the surface. Surface of the composite oxide is slightly Zn-deprived comparing to the bulk Zn/Zr ratio,[35] and there is a measurable effect on the modification of the surface acidity of ZrO_2 by the presence of ZnO. Intimate contact between the ZnO and ZrO_2 phases occurs as found by X-ray photoelectron spectroscopy (XPS), which leads to a modified surface chemistry of the composite $ZnZrO_x$ oxide beyond merely physical mixing.[31] With moderate amounts of ZnO addition (Zn:Zr = 1:10), the $ZnZrO_x$ mixture is able to maintain the homogeneous mixing of ZnO in ZrO_2 (Zn:Zr = 1:13) after NaCN leaching of the weakly bound gold ($x[OH]^- + [AuCl_4]^- \rightarrow x[Cl]^- + [AuCl_{4-x}OH_x]^-$), and still retains highly dispersed ZnO species with a lot of anchoring points for the gold atoms. Addition of gold was conducted by the anion-adsorption method[36] adapted from Lessard et al.[17] The $ZnZrO_x$ composite oxide with higher point of zero charge than pure ZrO_2 is more positively charged and releases more $[OH]^-$ in the aqueous phase to exchange with the gold precursor $[AuCl_4]^-$. The negatively charged Au precursor group binds tightly with the positively charged support surface, and prevents the agglomeration of Au atoms with protection from the ligands. The designated 1 wt.% gold loading was successfully achieved on $Zn_1Zr_{10}O_x$ with half of the gold (0.5 wt.%) remaining atomically dispersed after the NaCN leaching step. Heat treatment in oxidizing atmosphere ($2\%O_2$/He) at 300°C is required to pin the dispersed Au onto the support prior to NaCN leaching. For comparison, when the same synthesis method was used on pure ZrO_2 with 1 wt.% gold loading, agglomeration of the gold as nanoparticles took place after the heat treatment with only ~33% of the gold remaining atomically bound after the NaCN leaching step.[31]

The detailed synthesis technique for the atomically dispersed gold anchored on titania has been reported elsewhere.[16] In brief, a 4.8 wt.% Au/TiO_2 (anatase, from Millenium, ~300 m^2/g) made by DP prior to calcination was used as the starting material. Typically, 150 mL of $HAuCl_4$ aqueous solution was added into a 250 mL water suspension of 5 g titania. After stirring the slurry for 1 h, 1 mol/L of $(NH_4)_2CO_3$ solution was slowly added to keep the pH around 8. The slurry was heated to 343 K and aged for 1 h. The fresh samples were obtained by filtering the slurry, continuous washing with 70°C water, and then drying in vacuum at room temperature (RT) for 8–10 h. A UV chamber (365 nm, 10 mW/cm^2, Spectronics Corp.) was used for the irradiation of the samples. A slurry of 300 mg fresh sample and 50 mL liquid carrier medium (95% ethanol was used here) was poured into a cylindrical glass container (purged with N_2) and subjected to agitation for 15 min. During the UV treatment at RT, the reactor was placed in the middle of the chamber 2 cm away from the lamp. The powder sample was filtered and washed with DI water afterwards, and was fully dried in dark vacuum overnight. The dried powder was calcined in air at 200°C for 2 h to obtain the as-prepared 4.8 wt.% Au/TiO_2 parent sample. 0.05 wt.% NaCN solution (~pH 12) was used for gold leaching from the parent catalyst. About 300 mg of sample would be treated in each batch with continuous oxygen sparging, which lasted for 15 min until the color of the slurry was stabilized. The leached sample, 1.1 wt.% Au/TiO_2, was washed with DI water and dried at RT, and kept under vacuum in the dark.

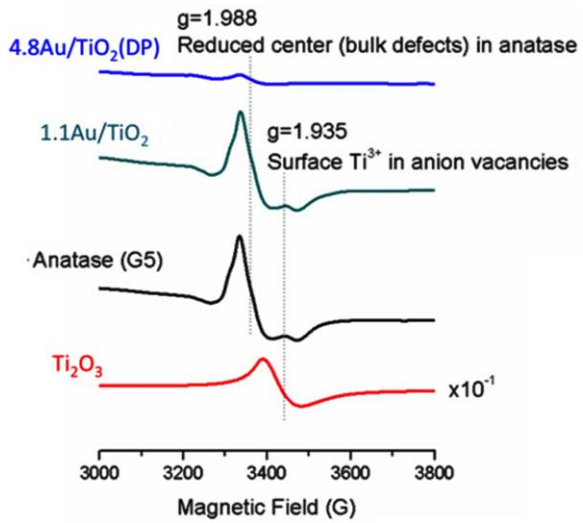

Figure 2. EPR spectra of the gold/titanium oxide samples collected at 120 K at ambient conditions.

All samples were stored in vacuum in the dark before testing. [Color figure can be viewed in the online issue, which is available at wileyonlinelibrary.com.]

Electron paramagnetic resonance spectroscopy (EPR) was used to probe the structural environment of paramagnetic unpaired electrons in the titanium oxides. 10 mg of sample were loaded in the quartz flow cells for the EPR measurements. Before these measurements, the samples were kept in the dark at RT for 72 h. The X-band (9 GHz) EPR spectra were recorded at 120 K in ambient atmosphere with a Bruker EMX EPR spectrometer. The magnetic field was swept from 2000 to 5000 Gauss. The location and the intensity of g factors were determined by Bruker's WINEPR program based on $h\nu = g\beta H$, where h is Planck's constant, H is the applied magnetic field, and β is the Bohr magneton. Center field for $g = 2.00$ is 3350 Gauss. A significant amount of both bulk Ti^{3+} defects ($g = 1.988$) and surface Ti-rich structures (Ti^{3+} associated with surface oxygen vacancies, $g = 1.935$)[37] were observed for the bare titanium oxides supports, as indicated by the peak of the paramagnetic unpaired electrons in the EPR spectra (Figure 2). For $4.8Au/TiO_2$, air calcination at 473 K for 2 h before UV treatment diminished the unpaired d-orbital electrons in Ti^{3+} that give rise to the EPR signal. However, when gold was atomically anchored on the titania surface (e.g., in $1.1Au/TiO_2$), there was a mutual stabilizing effect for the surface Ti^{3+}- rich site. Recent computational chemistry studies predict that such atop Au-O-Ti^{3+} site is energetically favorable.[38,39] Without a significant amount of gold (e.g. $1.1Au/TiO_2$) strongly interacting with the surface Ti^{3+}- rich site through −O bonds, the anatase vacancies were healed in

Table 1. SRM Reaction Rates[a] on Atomically Dispersed Gold Catalysts and Rescaling of Reaction Rates Based on the Amount of Au Atoms and Active –OH Groups

Sample	1.0 wt.% $Au/Zn_1Zr_8O_x$	1.0 wt.% $Au/Zn_1Zr_{13}O_x$	4.8 wt.% Au/TiO_2
Reference		31	16
Surface Zn:Zr ratio	1:7	1:35	-
S_{BET} (m^2/g)	79	97	270
Gold loading after leaching (wt.%)	0.5	0.5	1.1
Percent of Au retained (wt.%)	48.1	53.2	20
Percent of Zn retained (wt.%)	40	90	–
CO_2 production rate[b] at 240°C ($\mu mol/s/g_{cat}$)	0.15	0.14	0.26
TOF(Au)[c] at 240°C (s^{-1})	9.9×10^{-4}	9.5×10^{-4}	8.4×10^{-4}
−OH group ($\mu mol/g$)[d]—parent	684	739	549
−OH group ($\mu mol/g$)[d]—leached	333	635	544

[a]SRM reaction rate was measured for $CH_3OH/H_2O/He$ gas mixtures of molar ratio of 2/2.6/95.4; flow rate 20 cc/min, GHSV = 13,600/h.
[b]μmol of CO_2 produced per gram of catalyst per second.
[c]Gram of CO_2 produced per gram of gold per second.
[d]μmol of –OH groups per gram of catalyst up to 400°C, measured by CO-TPR[16,31]; for leached samples, the residual amount of –OH is shown.

the oxidative atmosphere as shown for $4.8Au/TiO_2$. Although the $4.8Au/TiO_2$ sample has four times higher gold content compared with the leached sample, the DP technique is less effective to build the stable Au-O-Ti^{3+} sites. Without UV treatment, gold forms NPs that bind weakly to the support surfaces, and the gold-titanium interaction through the –O- bonds is not established. According to the EPR analysis and the activity data, the WGS-active gold sites are the isolated atoms stably anchored on the titania sites. Through the –O-Ti^{3+} bonds, the cationic gold species was stabilized on the catalyst surface. In our previous work, it was shown clearly by XANES and XPS that these active gold sites being atomically anchored on the titanium oxide surfaces are positively charged due to the surrounding –O- bonds.[16]

Atomically Dispersed Supported Gold Catalysts for the SRM Reaction

The current generation of low-temperature (80°C) proton exchange membrane fuel cells requires CO-free hydrogen for maximum power density and to avoid degradation by the poisoning of the anode electrocatalyst by CO.[40] Among feed stocks for on-site H_2 production, methanol is very attractive due to its ready availability, high H:C ratio (4:1), and absence of C-C bonds. The SRM reaction (Rxn. 1) gives the highest H_2 yield among all the methanol-reforming (partial oxidation, autothermal) reactions. The SRM reaction may occur in a two-step series depending on the temperature and type of catalyst used as shown by methanol decomposition (Rxn. 2), followed by the WGS (Rxn. 3).[41–43] High temperature favors the formation of CO via the reverse water gas shift reaction, hence, it is important to operate the SRM at low temperatures.[44] Selective catalysts that do not catalyze the CO formation via Rxn. 2 are desirable as these do not include (and thus are not limited by the thermodynamic equilibrium of) Rxn. 3 as part of the SRM reaction pathway.[45]

$$CH_3OH + H_2O \leftrightarrows CO_2 + 3H_2 \quad \Delta H_r = 49.7 kJmol^{-1} \qquad (1)$$

$$CH_3OH \leftrightarrows CO + 2H_2 \quad \Delta H_r = 90.2 kJmol^{-1} \qquad (2)$$

$$CO + H_2O \leftrightarrows CO_2 + H_2 \quad \Delta H_r = -41.2 kJmol^{-1} \qquad (3)$$

The SRM reaction mechanism is believed to involve two different pathways on different catalyst surfaces. The first step upon adsorption of methanol is the formation of methoxy, adsorbed through the -O end; this may or may not lead to formaldehyde formation and stabilization on the surface. In the case where formaldehyde is formed, the intrinsic reason for the pathway difference is due to two distinct adsorption forms of formaldehyde as a reaction intermediate. The Iwasa group[46] described these two ways of formaldehyde adsorption as η^1(O)- and η^2(C,O)-form. By η^1(O)-adsorption, HCHO is adsorbed linearly on the catalyst surface, followed by a nucleophilic addition of water, and finally transformed into hydrogen and carbon dioxide via formic acid. In contrast, for the η^2(C,O)-adsorption, HCHO is bridged to the surface with C,O both bound onto the surface. The C-H bonds are easily broken when temperature increases, yielding hydrogen and carbon monoxide through decarbonylation of HCHO.[46–48] While the Pt group metals catalyze the Rxn 2, 3 pathway, Cu and Au catalyze the direct SRM reaction, involving HCHO in η^1(O)- configuration as an intermediate.[47]

Previous work by Yi et al.[25,29,49] and Boucher et al.[49] has identified methyl formate as a reaction intermediate during dynamic temperature-programmed surface reaction (TPSR) of H_2O-free methanol over supported Au catalysts on CeO_2 and ZnO.[25,29,30,49] This is the product of partial oxidation of methanol over oxidized gold species as demonstrated independently and for differently prepared gold catalysts, including bulk nanoporous gold alloy with residual silver, by the Friend group.[27,50–52] The formation of methyl formate is evidence of the oxidative self-coupling of methanol taking place on all these (oxidized) gold catalysts, whether supported or unsupported. The apparent activation energy of the SRM reaction on both Au/CeO_2 and Au/ZnO was measured as 110 ± 5 kJ/mol, indicative of same structurally gold active sites in these two systems. A strong shape effect of the supports was found, but this is indirect,[29] important only insofar as the number of anchoring points each shape provides to stabilize the atomic Au-O_x species. Deng et al.[14,53] have demonstrated the exclusive presence of isolated Au-O_x species in the NaCN-leached Au/CeO_2 sample by XANES/EXAFS measurements. In the case of the Au/ZnO system, the atomically dispersed gold species could only be imaged by ac-HAADF/STEM, in the presence of other gold structures, while XAS spectroscopy was ambiguous due to the overlapping of the excitation of Au and Zn. These limitations were overcome by the two new systems containing only gold atoms, and examined here as catalysts for the SRM reaction.[31]

A composite oxide with nominal composition of $Zn_1Zr_{10}O_x$, prepared by the carbon hard-template method had a bulk

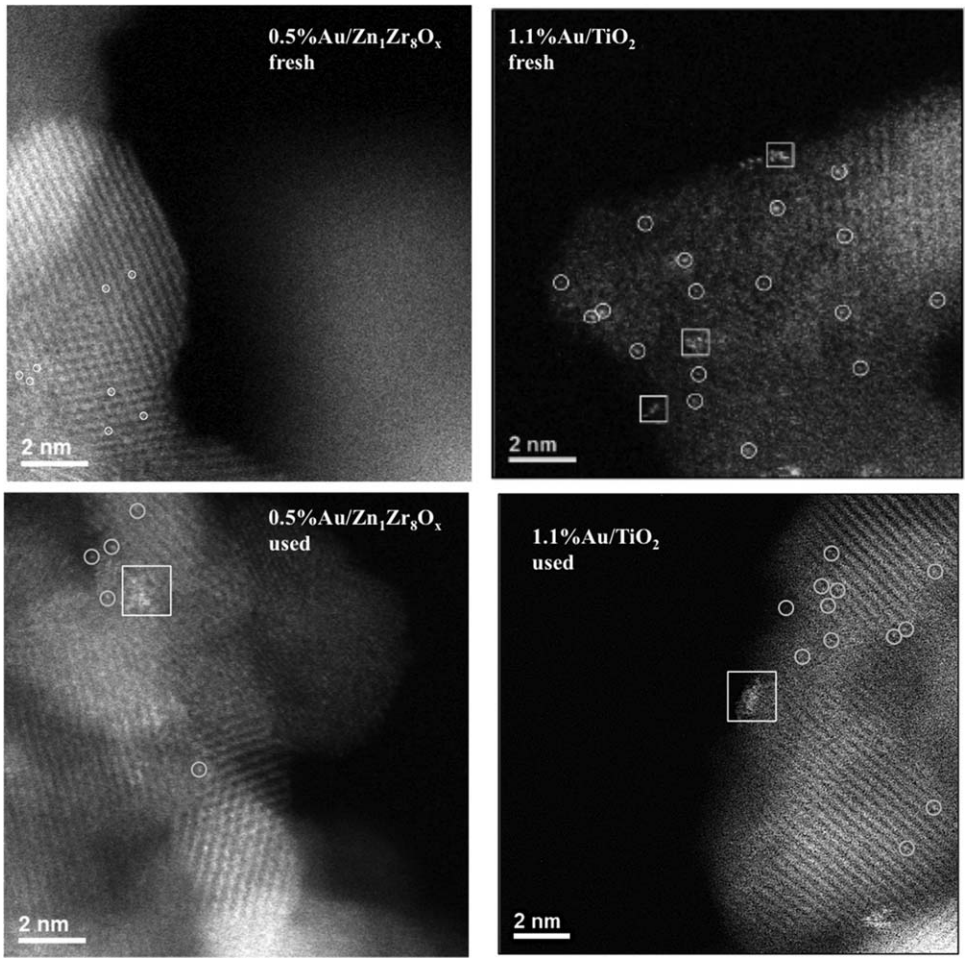

Figure 3. ac-HAADF/STEM images of fresh and used (in 2%:2.6%:95.4%=CH_3OH: H_2O: He SRM condition up to 400°C for $Au/Zn_1Zr_8O_x$ and 250°C for Au/TiO_2) gold catalysts.

The circles are drawn around isolated gold atoms, and the squares around closer spaced, but still distinct gold atoms.

composition of Zn:Zr = 1:8 as measured by inductively coupled plasma ion emission spectroscopy (ICP/IES). NaCN-leaching (0.05 wt.% NaCN aqueous solution, pH ≥ 12, r.t.) of bare $Zn_1Zr_8O_x$ composite oxide dissolves only part of the ZnO, leaving the bulk composition as $Zn_1Zr_{13}O_x$, which corresponds to the amount of ZnO the ZrO_2 domains can interact with, after removal of the excess amount of ZnO. The surface Zn:Zr composition and BET surface area of the two supports are listed in Table 1. Addition of 1wt.% gold to the two supports was achieved with the aforementioned anion adsorption method. NaCN leaching of 1 wt.% $Au/Zn_1Zr_8O_x$ and 1 wt.% $Au/Zn_1Zr_{13}O_x$ removed 52% and 47% of the deposited gold

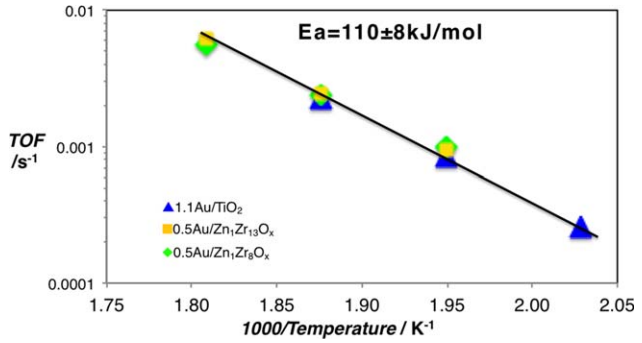

Figure 4. Arrhenius plot of the SRM-TOF on leached Au/TiO_2 and $Au/ZnZrO_x$ samples.

TOF was calculated by the CO_2 production rate per gold atom basis (2%CH_3OH, 2.6%H_2O, balance He, total flow rate = 20 mL/min; 100 mg catalyst loading; Temperature between 280°C and 220°C with 75 min holding at each set temperature). [Color figure can be viewed in the online issue, which is available at wileyonlinelibrary.com.]

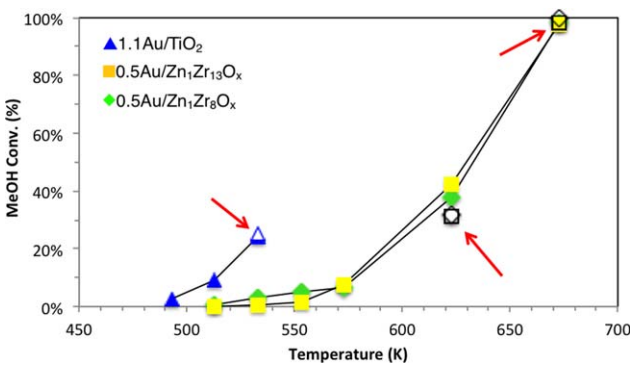

Figure 5. Stability test of Au/TiO_2 and $Au/ZnZrO_x$ samples in steady-state SRM.

2%CH_3OH, 2.6%H_2O, balance He, 100 mg catalyst loading. Total flow rate = 50 mL/min for $Au/ZnZrO_x$ samples and 20 mL/min for Au/TiO_2. Solid symbols represent the 1st-cycle results, open symbols represents the 2nd-cycle results. [Color figure can be viewed in the online issue, which is available at wileyonlinelibrary.com.]

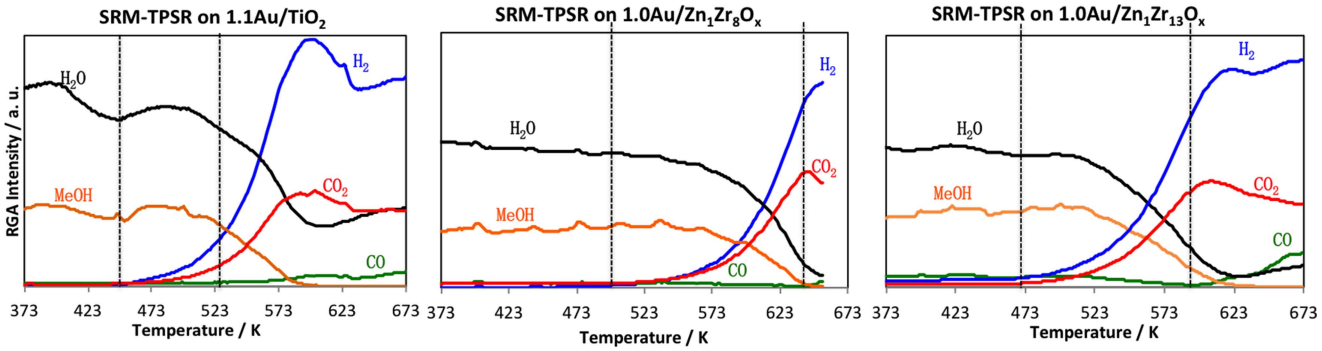

Figure 6. Temperature-programmed surface reaction of SRM on Au/TiO_2 and $Au/ZnZrO_x$ samples with comparable gold loading (~1 wt.%) (2%CH_3OH, 2.6%H_2O, balance He, total flow rate = 50 mL/min, GHSV = 34,000/h; 100 mg catalyst loading; Temperature increases linearly from 30 to 400°C in 3 h).

[Color figure can be viewed in the online issue, which is available at wileyonlinelibrary.com.]

and ~60% and 10% of zinc, respectively, (Table 1). For the Au/TiO_2 sample, NaCN leaching left 1.1 wt.% gold (4.8 wt.% of gold in the parent sample) intact on the surface. The residual gold is atomically dispersed as shown in the ac-HAADF/STEM micrographs (Figure 3). A significant amount of regenerable surface –OH groups were detected on both Au/TiO_2 and $Au/ZnZrO_x$ by cyclic CO-TPR (Table 1). The WGS activity of both gold and platinum catalysts was reported to correlate linearly with the regenerable surface –OH groups[23,24]; so the amount of these –OH groups can be used as a predictor of the WGS activity of the catalysts in the same temperature window shown in Table 1.

To verify whether the intrinsic activity of the atomically dispersed gold is the same on these as on previously used supports, steady state SRM tests were run on each of the three leached samples containing only gold atoms, namely; 1.1 wt.% Au/TiO_2, 0.5 wt.% $Au/Zn_1Zr_8O_x$, and 0.5wt.%$Au/Zn_1Zr_{13}O_x$. The gaseous mixture of CH_3OH/H_2O/He (2%/2.6%/95.4%) was passed through a fixed bed of 100 mg catalyst at a total flow rate of 20 mL/min, corresponding to gas hourly space velocity of 13,600/h. The reaction temperature was held constant for 90 min at each step shown in Figure 4, and conversion of methanol was kept <25% to measure rates

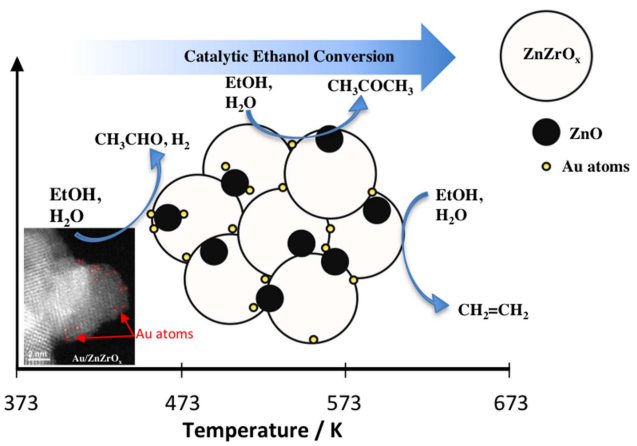

Scheme 1. Ethanol conversion scheme on Au species and $ZnZrO_x$ supports as a function of temperature.

Reprinted with permission from Ref 35, Copyright 2015 American Chemistry Society. [Color figure can be viewed in the online issue, which is available at wileyonlinelibrary.com.]

in the kinetic regime. The turnover frequency (TOF) of SRM was calculated based on the CO_2 production rate per gram of gold atoms on the support. Similar TOF values were measured for all three samples with the same apparent activation energy of 110 ± 8 kJ/mol. This provides strong evidence that the intrinsic activity of the atomic gold species is the same on all supports. Also, the overall activity of the catalyst is directly proportional to the amount of the atomically dispersed gold on these different supports. Stability tests of the Au/TiO_2 and $Au/ZnZrO_x$ samples were conducted in steady-state SRM conditions (Figure 5). For the two $Au/ZnZrO_x$ samples, SRM temperature was first increased to 400°C and decreased step by step to 240°C, followed by a 2nd-cycle of temperature ramping back to 400°C and 350°C. Methanol conversion at 400°C was maintained the same on the two samples for the 2nd-cycle, and decreased by ~7% at 350°C. Milder conditions were used for the stability test on Au/TiO_2, where the temperature peaked at 260°C for the 1st-cycle of steady-state SRM, and the same methanol conversion was observed at 260°C for the 2nd-cycle. Overall, the gold samples were able to maintain satisfactory stability with temperature ramping under realistic SRM conditions.

SRM on 1.1 wt.%Au/TiO_2, 1 wt.%$Au/Zn_1Zr_8O_x$, and 1 wt.% $Au/Zn_1Zr_{13}O_x$, was also performed in dynamic mode (Figure 6) to study the catalyst selectivity as a function of temperature. Wide temperature windows of CO-free methanol conversion were found on all three gold-containing samples, indicating that the direct SRM reaction mechanism does not involve neither the methanol decomposition nor the WGS reaction. Thus, similar to Au/CeO_2 and Au/ZnO,[25,26,29,30] the gold species on TiO_2 and $ZnZrO_x$ catalyze the same reaction pathway with methyl formate as the reaction intermediate. The reverse WGS reaction starts to occur when the temperature exceeds 325–375°C, leaving the low to intermediate temperature regions accessible for practical CO-free SRM operation.

Atomically Dispersed Supported Au Catalysts for the Ethanol Dehydrogenation Reaction

The single-atom supported gold species were shown above as the catalytic sites for the SRM reaction through a first methoxy species adsorbed linearly on the gold atom then formaldehyde in η^1(O) configuration, further catalyzing the coupling reaction with another methanol molecule and the methyl formate production under oxidative conditions. This

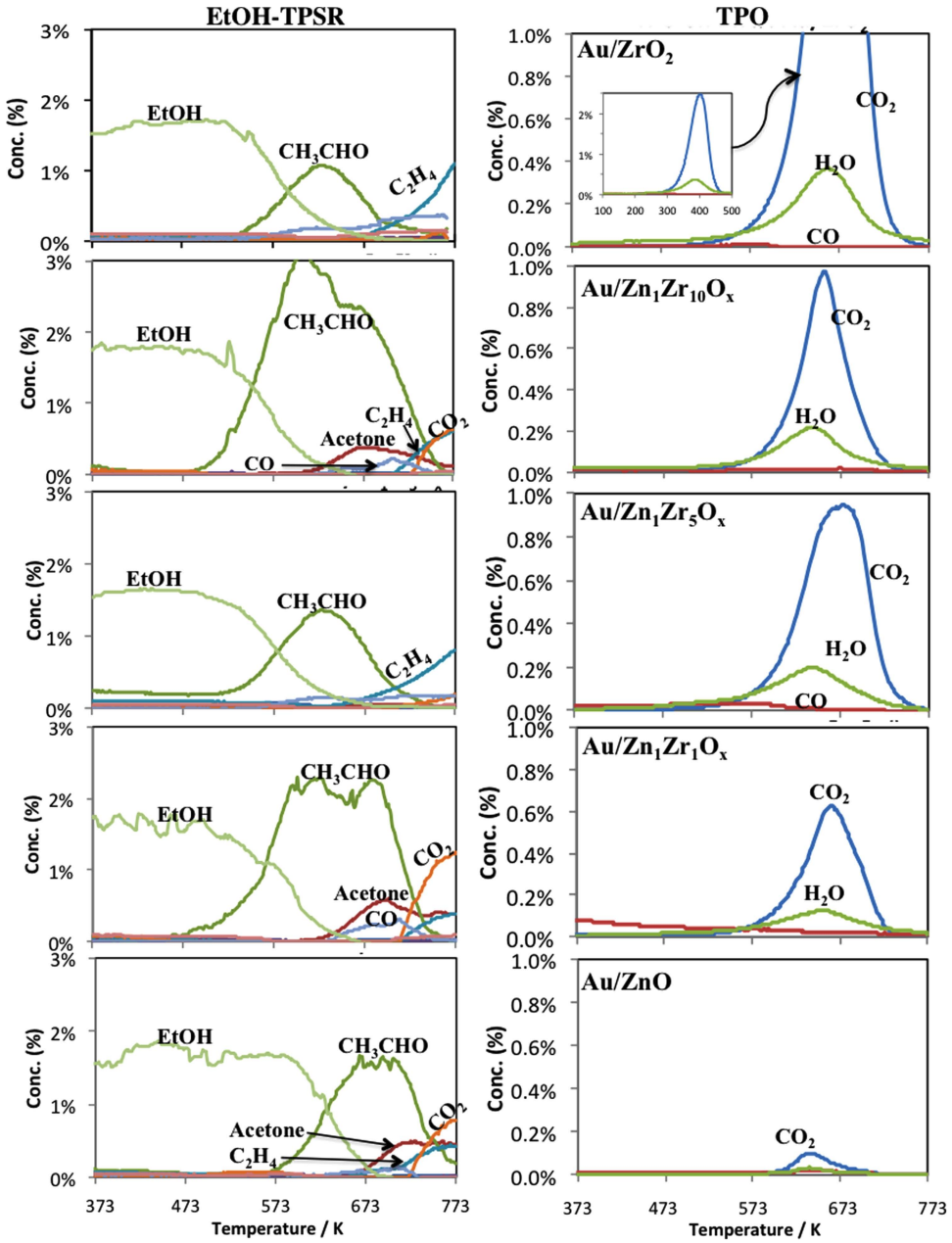

Figure 7. Ethanol-TPSR on supported gold catalysts (2%CH3CH2OH balance in He, total flow rate = 50 mL/min; Temperature increases linearly from 30°C to 500°C in 4 h; 100mg catalyst loading; WHSV= 111.5 gEtOH/(gAu•h)).

Reprinted with permission from Ref 35, Copyright 2015 American Chemistry Society [Color figure can be viewed in the online issue, which is available at wileyonlinelibrary.com.]

scheme may be the same for higher alcohols. Indeed, this was reported for nanoporous gold and oxygen-activated Au(111) by the group of Madix and Friend,[27,50] as was the reaction of higher alcohols with methanol to make the corresponding mixed esters in partial oxidation conditions. From the point of view of further fundamental understanding of the alcohol interactions with gold, we examine here the nonoxidative dehydrogenation of ethanol to acetaldehyde and hydrogen. If this reaction is catalyzed by the isolated atomic gold species, it will be a significant finding, especially in view of green chemicals/hydrogen production from biomass-derived ethanol.

During the past decade, the production of hydrogen from bio-ethanol through the ethanol steam reforming (ESR) reaction has been intensively studied, especially for application to fuel cells.[54,55]

$$C_2H_5OH + 3H_2O \rightarrow 2CO_2 + 6H_2 \quad (4)$$

Thermodynamic equilibria in the temperature range of 100°C–1000°C predict the main products of ESR to be the ethanol cracking products like CO, CH_4, CO_2, and H_2. However, products of ethanol dehydration and dehydrogenation are commonly detected in practical reaction systems in this temperature range, suggesting that these reactions are kinetically controlled and occur faster before steam reforming light off.[56] Therefore, bioethanol is also a candidate feedstock to value-added chemicals,[57] such as the production of acetaldehyde on

Au-based bimetallic catalysts,[58,59] and production of acetone[60–64] and isobutene[32,65,66] on metal oxide catalysts. Catalytic conversion of ethanol involves cascade of elementary reactions. Fundamental work by Mavrikakis and Barteau[67] has discussed the thermal stability and configuration of C_1 and C_2 alcohol adsorption on group VIII (Ni, Pd, Pt, Ru) and group IB metals (Cu, Ag) as summarized below

$$\text{Alcohol} \rightarrow \text{Alkoxide} \rightarrow \eta^1(\text{O}) \text{ or } \eta^2(\text{C, O}) - \text{surface}$$
$$- \text{bound aldehyde} \rightarrow \text{Acyl}$$

Formation of the aldehyde species requires rapid transfer of hydroxyl group hydrogen and α-hydrogen to adjacent basic oxygen.[68] The adsorption configuration of the aldehyde species depends primarily on the electronegativity of the metal surface, that is, η^1(O)-configuration occurs via carbonyl compound bonding with the surface through the oxygen lone pair orbital, acting as a Lewis base. Conversely, the η^2(C,O)-configuration occurs with back-donation of electrons from the metal to carbon in the carbonyl compound. Stability of the η^2-adsorption promotes decomposition of the adsorbates more than desorption as in the η^1-adsorption. At low (150–250°C) and intermediate temperatures (250–350°C), catalytic conversion of ethanol to value-added chemicals, like acetaldehyde and acetone, includes molecular adsorption of ethanol on the catalyst surface; scission of O-H bond to form ethoxide, followed by dehydrogenation of ethoxide to acetaldehyde (Rxn 5) and oxidation of acetaldehyde to acetone by mobile surface oxygen species (Rxn 6). Direct synthesis of acetone from ethanol[60–64] requires the synergistic interaction of multiple active sites, which calls for basic sites that catalyze the scission of the O-H bond of ethanol and regenerable mobile oxygen species on the surface from oxygen or steam

$$CH_3CH_2 - OH \rightarrow CH_3CHO + H_2 \quad (5)$$

$$2CH_3CHO + O^* \rightarrow CH_3COCH_3 + CO_2 + H_2 \quad (6)$$

Here, we used the Au/$ZnZrO_x$ catalyst for the low-temperature dehydrogenation of ethanol for acetaldehyde and hydrogen production (Scheme 1). A series of $ZnZrO_x$ with improved physical properties and different surface chemistry than either of the pure ZnO and ZrO_2 samples were used as

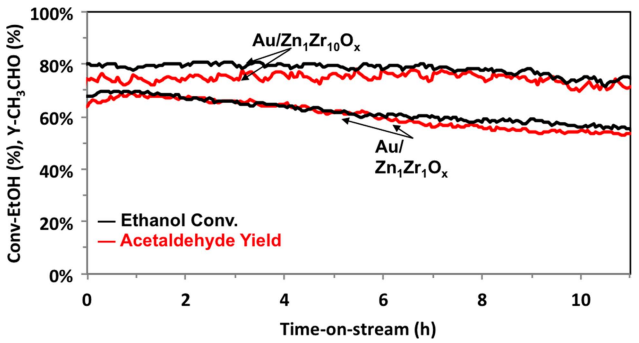

Figure 8. Stability tests (2%EtOH+2%H2O/He) on Au/$Zn_1Zr_{10}O_x$ and Au/$Zn_1Zr_1O_x$, total flow rate = 50 mL/min, T=325°C for 11 h. Catalyst loading = 100mg, WHSV = 1.11 gEtOH/(gC_{at}•h).

Reprinted with permission from Ref 35, Copyright 2015 American Chemistry Society. [Color figure can be viewed in the online issue, which is available at wileyonlinelibrary.com.]

Table 2. Ethanol Dehydrogenation Rates on Parent and Leached Au/$ZnZrO_x$ Samples

Sample	L-Au/ $Zn_1Zr_1O_x$	L-Au/ $Zn_1Zr_{10}O_x$	Au/ $Zn_1Zr_1O_x$	Au/ $Zn_1Zr_{10}O_x$
EtOH conv.rate[a]	3.04	6.04	5.53	6.52
CH_3CHO prod.[b]	2.28	5.28	5.19	5.79
Residual Au %	54	58	–	–
Residual Zn %	88	78	–	–

[a]Ethanol conversion rate at 350°C in units of μmol s^{-1} g_{cat}^{-1}.
[b]Acetaldehyde production rate at 350°C in units of μmol s^{-1} g_{cat}^{-1}.

gold supports for the selective ethanol dehydrogenation reaction. Ethanol itself can serve as a probe molecule to titrate the modification of the ZrO_2 surface chemistry by ZnO-addition. Ethanol TPSR (EtOH-TPSR, 2%CH_3CH_2OH, balance in He) in the temperature range of 30°C–500°C on the fixed bed catalyst with mass spectrometry monitoring was performed to titrate the surface. Acidic sites on pure ZrO_2 primarily catalyze the undesired dehydration of ethanol to produce ethylene. With increased ZnO loading, production of ethylene monotonically decreases while production of acetaldehyde increases.[35] As shown in our previous work,[35] the intermediate temperature window (300–500°C) for the ethylene and acetaldehyde production overlaps on the bare $ZnZrO_x$ supports so that separation of the products is an issue. However, addition of 1 wt.% Au to the bare supports significantly changes the product distribution in the range of 200°C–400°C, and separates the temperature zones by lowering the acetaldehyde light off temperature to ~200°C while shifting the ethylene production to >400°C (Figure 7). Another issue in ethanol conversion is hydrocarbon (CH_x) and carbon deposition due to ethylene polymerization and the ethanol C-C bond cracking, which is a major cause for catalyst deactivation. Cofeeding of steam with ethanol could suppress the CH_x and carbon deposition with steam serving as a mild oxidant; however, supplying excess amount of steam would be energy consuming and hence undesirable for practical applications. Therefore, it is important to develop a catalyst system that is less prone to cause CH_x and carbon deposition in the first place. With the same amount of gold loading (~1 wt.%), we pushed the limit of the ethanol-TPSR reaction temperature to 500°C (2%CH_3CH_2OH balance in He) followed by temperature-programmed oxidation (TPO, 10%O_2 balance in He) of the used gold catalysts. CO_2 and H_2O production during TPO clearly indicates the CH_x fragment deposition during ethanol-TPSR on all spent samples. Moreover, there exists a trend of increasing amount of CH_x fragment deposition on the more acidic supports. This finding corroborates our understanding of oxide supports by ethanol titration; namely that ZnO-passivation of the surface acidity suppresses the ethylene production.

Stability testing of two gold catalysts at a moderately high temperature (325°C) was performed for 11 h on-stream (Figure 8) with continuous monitoring of the products by mass spectrometry. The acetaldehyde yield was closely matched to the ethanol conversion, showing that no side reactions occurred up to 325°C. The inclusion of water up to 325°C has no effect on the chemistry, that is, the water does not further convert ethanol to oxygenated products, like acetic acid and ethyl acetate, which would be the dominant products when ethanol and O_2 are cofed over Au/ZSM5 catalysts.[69] ESR also does not take place at these temperatures. Thus, there is a wide (200–325°C) operating window for the selective production of

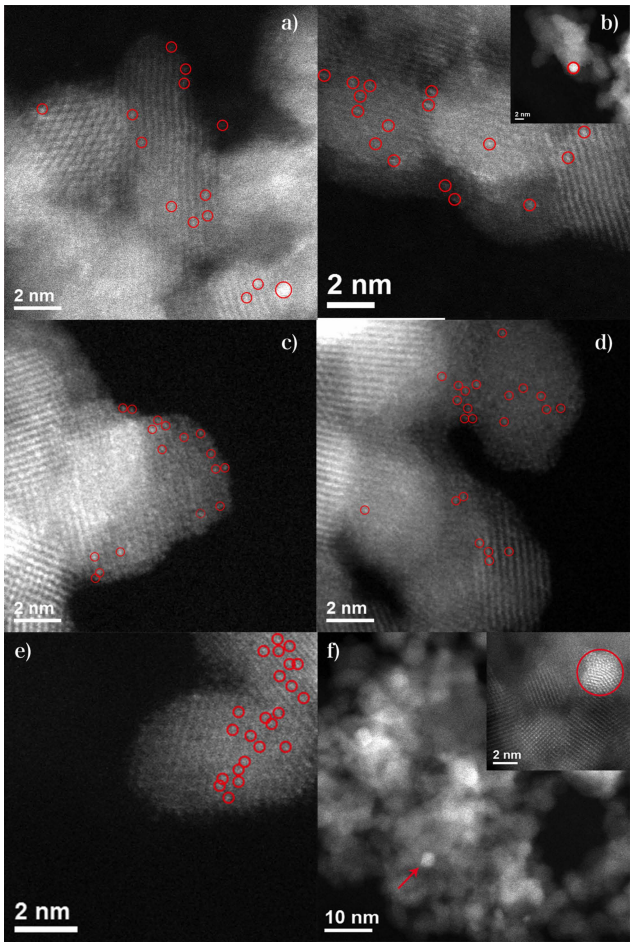

Figure 9. ac-HAADF-STEM of fresh parent samples. (a) $Au/Zn_1Zr_{10}O_x$, (b) $Au/Zn_1Zr_1O_x$; fresh leached samples (c) $Au/Zn_1Zr_{10}O_x$, (d) Au/Zn_1Zr_1Ox; and spent leached samples (e) $Au/Zn_1Zr_{10}O_x$, (f) $Au/Zn_1Zr_1O_x$ in steady-state ethanol dehydrogenation reaction (2% ethanol/2% steam/96% He) up to 673 K. Reprinted with permission from Ref 35.

acetaldehyde and hydrogen from ethanol in the presence of water over single-atom supported gold catalysts.

In summary, we have shown that the chemistry of gold is separate from that of the acidic/basic surface support and at low temperatures, ethanol dehydrogenation to acetaldehyde and hydrogen exclusively takes place on gold supported on $ZnZrO_x$. These active sites are the single-atom gold sites, checked by repeating the reaction on the leached $Au/ZnZrO_x$ samples. As shown in Table 2, catalyst activity and selectivity is maintained on L-$Au/Zn_1Zr_{10}O_x$ similar to the parent sample, whereas decreased activity was observed on L-$Au/Zn_1Zr_1O_x$. Although a similar amount of Au was leached from the two parent samples, a much higher amount of Zn was leached away from 1 wt.% $Au/Zn_1Zr_1O_x$, considering the higher Zn amount of $Zn_1Zr_1O_x$ in bulk. Previous research on Au/ZnO system has demonstrated that strong interaction between Au atoms and the $ZnZrO_x$ support is through the Au-O_x-ZnO linkages,[70] where oxygen defects occur on the highly dispersed ZnO,[29] hence the loss of ZnO anchoring sites affects the activity. Addition of Zn to ZrO_2 with 1:1 ratio exceeds the critical Zn amount that ZrO_2 is able to accommodate without forming isolated ZnO clusters. Removal of Zn at ~12% from $Zn_1Zr_1O_x$ has most likely dissolved the isolated ZnO clusters and destabilized Au-O_x-ZnO species, so that a lower catalyst activity was observed on the L-$Au/Zn_1Zr_1O_x$ than on L-$Au/Zn_1Zr_{10}O_x$. This argument agrees with the gold aggregation detected only on the spent L-$Au/Zn_1Zr_1O_x$ but not on the spent L-$Au/Zn_1Zr_{10}O_x$ after steady-state reaction up to 400°C for 75 min (Figure 9) illustrated by STEM. This finding can guide the design of catalysts with efficient use of Au and Zn additives to avoid "over design." More details about the identification and quantitation of the active sites for the low-temperature ethanol dehydrogenation on gold can be found in a recent report.[35]

Conclusion

In this work, we have presented a brief account of recently studied single-atom gold catalysts on different supports. We show how not only the WGS reaction, but also the SRM and ethanol dehydrogenation reactions take place on single-site supported gold species. The atomic gold is cationic anchored on the oxide supports through –O bonds. The support has only an indirect effect on the reaction, through the number of anchoring sites it can provide to the gold atom. For each reaction, there is a distinct apparent activation energy irrespective of the support used. The latter serves to disperse and stabilize the gold atoms, hence its physical properties are important to maximize its capacity to anchor gold atoms and hence the overall activity. We also showed the importance of catalyst preparation method to increase the interaction of gold with the support. UV radiation-assisted deposition was used for the 1 wt.% atomic Au/TiO_2 synthesis, and a combination of the anion-adsorption of gold and carbon hard-template technique was used for the $Au/ZnZrO_x$ synthesis to disperse ZnO and associate them strongly with zirconia. SRM reactions were included to demonstrate the key idea that gold atom–centered Au-O_x sites on an oxide support catalyze these reactions equally well, regardless of the support being used. The $Au/ZnZrO_x$ material was shown as an effective, highly selective and stable catalyst for ethanol dehydrogenation to acetaldehyde and hydrogen over a wide temperature window with lightoff at ~200°C. These findings pave the way for new and exciting applications of atomic dispersions of gold (and other metals) for a variety of reactions with flexible choice of a support, such that the precious metal utilization is maximized.

Acknowledgments

The authors acknowledge the financial support of this work by the U.S. Department of Energy under Grant No. DE-FG02-05ER15730. C.W. thanks Dr. Y. Zhang and Dr. C. Settens at the Center for Material Science and Engineering of MIT; and Dr. H. Lin at the Center for Nanoscale Systems of Harvard University for their assistance with sample characterization. The authors are also grateful to Dr. L. F. Allard of the Oak Ridge National Laboratory for his assistance with the ac-HAADF/STEM work.

Literature Cited

1. Cha DY, Parravano G. Surface reactivity of supported gold: I. Oxygen transfer between CO and CO2. *J Catal.* 1970;18(2):200–211.
2. Haruta M, Kobayashi T, Sano H, Yamada N. Novel gold catalysts for the oxidation of carbon monoxide at a temperature far below 0°C. *Chem Lett.* 1987;16(2):405–408.

3. Haruta M, Tsubota S, Kobayashi T, Kageyama H, Genet MJ, Delmon B. Low-Temperature Oxidation of CO over Gold Supported on TiO2, α-Fe2O3, and Co3O4. *J Catal*. 1993;144(1):175–192.
4. Haruta M, Yamada N, Kobayashi T, Iijima S. Gold catalysts prepared by coprecipitation for low-temperature oxidation of hydrogen and of carbon monoxide. *J Catal*. 1989;115(2):301–309.
5. Liu W, Flytzanistephanopoulos M. Total oxidation of carbon monoxide and methane over transition metal fluorite oxide composite catalysts: I. catalyst composition and activity. *J Catal*. 1995;153(2):304–316.
6. Liu W, Flytzanistephanopoulos M. Total oxidation of carbonmonoxide and methane over transition metal fluorite oxide composite catalysts: II. catalyst characterization and reaction-kinetics. *J Catal*. 1995;153(2):317–332.
7. Fu Q, Weber A, Flytzani-Stephanopoulos M. Nanostructured Au/CeO2 catalysts for low-temperature water-gas shift. *Catal Lett*. 2001;77(1–3):87–95.
8. Deng W, Jesus JD, Saltsburg H, Flytzani-Stephanopoulos M. Low-content gold-ceria catalysts for the water–gas shift and preferential CO oxidation reactions. *Appl Catal A Gen*. 2005;291(1–2):126–135.
9. Fu Q, Saltsburg H, Flytzani-Stephanopoulos M. Active Nonmetallic Au and Pt species on ceria-based water-gas shift catalysts. *Science*. 2003;301(5635):935–938.
10. Flytzani-Stephanopoulos M, Gates BC. Atomically dispersed supported metal catalysts. *Annu Rev Chem Biomol Eng*. 2012;3(1):545–574.
11. Flytzani-Stephanopoulos M. Gold atoms stabilized on various supports catalyze the water–gas shift Reaction. *Acc Chem Res*. 2014; 47(3):783–792.
12. Thomas JM. The concept, reality and utility of single-site heterogeneous catalysts (SSHCs). *PCCP*. 2014;16(17):7647–7661.
13. Deng W, Frenkel AI, Si R, Flytzani-Stephanopoulos M. Reaction-relevant gold structures in the low temperature water-gas shift reaction on Au-CeO2. *J Phys Chem C*. 2008;112(33):12834–12840.
14. Deng W, Carpenter C, Yi N, Flytzani-Stephanopoulos M. Comparison of the activity of Au/CeO2 and Au/Fe2O3 catalysts for the CO oxidation and the water-gas shift reactions. *Top Catal*. 2007;44(1): 199–208.
15. Allard LF, Borisevich A, Deng W, Si R, Flytzani-Stephanopoulos M, Overbury SH. Evolution of gold structure during thermal treatment of Au/FeOx catalysts revealed by aberration-corrected electron microscopy. *J Electron Microsc*. 2009;58(3):199–212.
16. Yang M, Allard LF, Flytzani-Stephanopoulos M. Atomically dispersed Au-(OH)x species bound on titania catalyze the low-temperature water-gas shift reaction. *J Am Chem Soc*. 2013;135(10): 3768–3771.
17. Lessard JD, Valsamakis I, Flytzani-Stephanopoulos M. Novel Au/La2O3 and Au/La2O2SO4 catalysts for the water-gas shift reaction prepared via an anion adsorption method. *Chem Commun*. 2012; 48(40):4857–4859.
18. Si R, Flytzani-Stephanopoulos M. Shape and crystal-plane effects of nanoscale ceria on the activity of Au-CeO2 catalysts for the water-gas shift reaction. *Angew Chem*. 2008;120(15):2926–2929.
19. Zugic B, Zhang S, Bell DC, Tao F, Flytzani-Stephanopoulos M. Probing the low-temperature water–gas shift activity of alkali-promoted platinum catalysts stabilized on carbon supports. *J Am Chem Soc*. 2014;136(8):3238–3245.
20. Zugic B, Bell DC, Flytzani-Stephanopoulos M. Activation of carbon-supported platinum catalysts by sodium for the low-temperature water-gas shift reaction. *Appl Catal B Environ* 2014; 144:243–251.
21. Yang M, Liu J, Lee S, Zugic B, Huang J, Allard LF, Flytzani-Stephanopoulos M. A common single-site Pt(II)–O(OH)x– species stabilized by sodium on "active" and "inert" supports catalyzes the water-gas shift reaction. *J Am Chem Soc*. 2015;137(10):3470–3473.
22. Wang Y, Zhai Y, Pierre D, Flytzani-Stephanopoulos M. Silica-encapsulated platinum catalysts for the low-temperature water-gas shift reaction. *Appl Catal B Environ* 2012;127:342–350.
23. Zhai Y, Pierre D, Si R, Deng W, Ferrin P, Nilekar AU, Peng G, Herron JA, Bell DC, Saltsburg H, Mavrikakis M, Flytzani-Stephanopoulos M. Alkali-stabilized pt-ohx species catalyze low-temperature water-gas shift reactions. *Science*. 2010;329(5999): 1633–1636.
24. Yang M, Li S, Wang Y, Herron JA, Xu Y, Allard LF, Lee S, Huang J, Mavrikakis M, Flytzani-Stephanopoulos M. Catalytically active Au-O(OH)x- species stabilized by alkali ions on zeolites and mesoporous oxides. *Science*. 2014;346(6216):1498–1501.
25. Yi N, Si R, Saltsburg H, Flytzani-Stephanopoulos M. Active gold species on cerium oxide nanoshapes for methanol steam reforming and the water gas shift reactions. *Energy Environ Sci*. 2010;3(6):831–837.
26. Yi N, Si R, Saltsburg H, Flytzani-Stephanopoulos M. Steam reforming of methanol over ceria and gold-ceria nanoshapes. *Appl Catal B Environ* 2010;95(1–2):87–92.
27. Xu B, Liu X, Haubrich J, Friend CM. Vapour-phase gold-surface-mediated coupling of aldehydes with methanol. *Nat Chem*. 2010; 2(1):61–65.
28. Wittstock A, Zielasek V, Biener J, Friend CM, Bäumer M. Nanoporous gold catalysts for selective gas-phase oxidative coupling of methanol at low temperature. *Science*. 2010;327(5963):319–322.
29. Boucher MB, Goergen S, Yi N, Flytzani-Stephanopoulos M. 'Shape effects' in metal oxide supported nanoscale gold catalysts. *PCCP*. 2011;13(7):2517–2527.
30. Yi N, Boucher MB, Gittleson F, Zugic B, Saltsburg H, Flytzani-Stephanopoulos M. Hydrogen production from methanol over gold supported on ZnO and CeO2 nanoshapes. *J Phys Chem C*. 2011; 115(4):1261–1268.
31. Wang C, Boucher M, Yang M, Saltsburg H, Flytzani-Stephanopoulos M. ZnO-modified zirconia as gold catalyst support for the low-temperature methanol steam reforming reaction. *Appl Catal BEnviron*. 2014;154–155:142–152.
32. Sun J, Zhu K, Gao F, Wang C, Liu J, Peden CHF, Wang Y. Direct Conversion of bio-ethanol to isobutene on nanosized ZnxZryOz mixed oxides with balanced acid-base sites. *J Am Chem Soc* 2011; 133(29):11096–11099.
33. Dulub O, Boatner LA, Diebold U. STM study of the geometric and electronic structure of ZnO(0001)-Zn, (000$\bar{1}$0)-O, (10$\bar{1}$0), and (11$\bar{2}$0) surfaces. *Surf Sci*. 2002;519(3):201–217.
34. Liu C, Sun J, Smith C, Wang Y. A study of ZnxZryOz mixed oxides for direct conversion of ethanol to isobutene. *Appl Catal A Gen*. 2013;467:91–97.
35. Wang C, Garbarino G, Allard LF, Wilson F, Busca G, Flytzani-Stephanopoulos M. Low-temperature dehydrogenation of ethanol on atomically dispersed gold supported on ZnZrOx. *ACS Catal*. 2015.
36. Regalbuto J. *Catalyst Preparation: Science and Engineering*, Florida, US: CRC Press, 2007.
37. Xiong L-B, Li J-L, Yang B, Yu Y. In the surface of titanium dioxide: generation, properties and photocatalytic application. *J Nanomater*. 2012;2012:13.
38. Okazaki K, Morikawa Y, Tanaka S, Tanaka K, Kohyama M. Electronic structures of Au on TiO2(110) by first-principles calculations. *Phys Rev B*. 2004;69(23):235404.
39. Matthey D, Wang JG, Wendt S, Matthiesen J, Schaub R, Lægsgaard E, Hammer B, Besenbacher F. Enhanced bonding of gold nanoparticles on oxidized TiO2(110). *science*. 2007;315 (5819):1692–1696.
40. Larminie J, Dicks A. *Fuel Cell Systems Explained*, *2nd ed*. Chichester, UK: Wiley, 2003.
41. Sa S, Silva H, Brandao L, Sousa JM, Mendes A. Catalysts for methanol steam reforming–A review. *Appl Catal. B Environ* 2010;99(1–2): 43–57.
42. Menegazzo F, Pinna F, Signoretto M, Trevisan V, Boccuzzi F, Chiorino A, Manzoli M. Highly dispersed gold on zirconia: characterization and activity in low-temperature water gas shift tests. *ChemSusChem*. 2008;1(4):320–326.
43. Matsumura Y, Ishibe H. High temperature steam reforming of methanol over Cu/ZnO/ZrO2 catalysts. *Appl Catal B Environ*. 2009;91(1–2):524–532.
44. Chorkendorff I, Niemantsverdriet JW. *Concepts of Modern Catalysis and Kinetics*, Gemany: WILEY-VCH, 2005.
45. Palo DR, Dagle RA, Holladay JD. Methanol steam reforming for hydrogen production. *Chem Rev*. 2007;107(10):3992–4021.
46. Iwasa N, Takezawa N. New supported Pd and Pt alloy catalysts for steam reforming and dehydrogenation of methanol. *Top Catal*. 2003; 22(3):215–224.
47. Iwasa N, Mayanagi T, Nomura W, Arai M, Takezawa N. Effect of Zn addition to supported Pd catalysts in the steam reforming of methanol. *Appl Catal A Gen* 2003;248(1–2):153–160.
48. Iwasa N, Mayanagi T, Ogawa N, Sakata K, Takezawa N. New catalytic functions of Pd–Zn, Pd–Ga, Pd–In, Pt–Zn, Pt–Ga and Pt–In alloys in the conversions of methanol. *Catal Lett*. 1998;54(3):119–123.
49. Yi N, Saltsburg H, Flytzani-Stephanopoulos M. Hydrogen production by dehydrogenation of formic acid on atomically dispersed gold on ceria. *ChemSusChem*. 2013;6(5):816–819.

50. Xu B, Haubrich J, Baker TA, Kaxiras E, Friend CM. Theoretical study of O-assisted selective coupling of methanol on Au(111). *J Phys Chem C*. 2011;115(9):3703–3708.
51. Xu B, Liu X, Haubrich J, Madix R, Friend C. Selectivity control in gold-mediated esterification of Methanol. *Angew Chem Int Ed*. 2009; 48(23):4206–4209.
52. Xu B, Haubrich J, Freyschlag CG, Madix RJ, Friend CM. Oxygen-assisted cross-coupling of methanol with alkyl alcohols on metallic gold. *Chem Sci*. 2010;1(3):310–314.
53. Deng W, Flytzani-Stephanopoulos M. On the issue of the deactivation of au-ceria and pt-ceria water-gas shift catalysts in practical fuel-cell applications13. *Angew Chem Int Ed*. 2006;45(14):2285–2289.
54. Deluga GA, Salge JR, Schmidt LD, Verykios XE. Renewable hydrogen from ethanol by autothermal reforming. *Science*. 2004; 303(5660):993–997.
55. Huber GW, Shabaker JW, Dumesic JA. Raney Ni-Sn Catalyst for H2 Production from biomass-derived hydrocarbons. *Science*. 2003; 300(5628):2075–2077.
56. Rabenstein G, Hacker V. Hydrogen for fuel cells from ethanol by steam-reforming, partial-oxidation and combined auto-thermal reforming: A thermodynamic analysis. *J Power Sources*. 2008; 185(2):1293–1304.
57. Sun J, Wang Y. Recent Advances in catalytic conversion of ethanol to chemicals. *ACS Catal*. 2014;4(4):1078–1090.
58. Redina EA, Greish AA, Mishin IV, et al. Selective oxidation of ethanol to acetaldehyde over Au–Cu catalysts prepared by a redox method. *Catal Today*. 2015;241, Part B:246–254.
59. Guan Y, Hensen EJM. Selective oxidation of ethanol to acetaldehyde by Au−Ir catalysts. *J Catal*. 2013;305:135–145.
60. Murthy RS, Patnaik P, Sidheswaran P, Jayamani M. Conversion of ethanol to acetone over promoted iron oxide catalysis. *J Catal*. 1988;109(2):298–302.
61. Nakajima T, Nameta H, Mishima S, Matsuzaki I, Tanabe K. A highly active and highly selective oxide catalyst for the conversion of ethanol to acetone in the presence of water vapour. *J Mater Chem*. 1994;4(6):853–858.
62. Nakajima T, Tanabe K, Yamaguchi T, Matsuzaki I, Mishima S. Conversion of ethanol to acetone over zinc oxide-calcium oxide catalyst optimization of catalyst preparation and reaction conditions and deduction of reaction mechanism. *Appl Catal*. 1989; 52(3):237–248.
63. Nishiguchi T, Matsumoto T, Kanai H, Utani K, Matsumura Y, Shen W-J, Imamura S, . Catalytic steam reforming of ethanol to produce hydrogen and acetone. *Appl Catal. A Gen*. 2005;279(1–2):273–277.
64. Rodrigues CP, Zonetti PC, Silva CG, Gaspar AB, Appel LG. Chemicals from ethanol-The acetone one-pot synthesis. *Appl Catal A Gen*. 2013;458(0):111–118.
65. Tago T, Konno H, Ikeda S, Yamazaki S, Ninomiya W, Nakasaka Y, Masuda T. Selective production of isobutylene from acetone over alkali metal ion-exchanged BEA zeolites. *Catal Today*. 2011;164(1): 158–162.
66. Tago T, Konno H, Sakamoto M, Nakasaka Y, Masuda T. Selective synthesis for light olefins from acetone over ZSM-5 zeolites with nano- and macro-crystal sizes. *Appl. Catal. A Gen*. 2011;403(1–2): 183–191.
67. Mavrikakis M, Barteau MA. Oxygenate reaction pathways on transition metal surfaces. *J Mol Catal A Chem*. 1998;131(1–3):135–147.
68. Wachs IE, Madix RJ. The oxidation of methanol on a silver (110) catalyst. *Surf Sci*. 1978;76(2):531–558.
69. Chen H, Jia X, Li Y, Liu C, Yang Y. Controlled surface properties of Au/ZSM5 catalysts and their effects in the selective oxidation of ethanol. *Catal Today*. 2015;256, Part 1:153–160.
70. Liu X, Liu M-H, Luo Y-C, Mou C-Y, Lin SD, Cheng H, Chen J-M, Lee J-F, Lin T-S, . Strong metal-support interactions between gold nanoparticles and ZnO nanorods in CO oxidation. *J Am Chem Soc*. 2012;134(24):10251–10258.

Manuscript received Sep. 3, 2015, and revision received Dec. 5, 2015.